

Cobalt–iridium impregnated zirconium-doped mesoporous silica as catalysts for the selective catalytic reduction of NO with ammonia

Ramón Moreno-Tost, Enrique Rodríguez Castellón, Antonio Jiménez-López*

*Departamento de Química Inorgánica, Cristalografía y Mineralogía (Unidad Asociada al ICP-CSIC),
Facultad de Ciencias, Universidad de Málaga, Campus de Teatinos, 29071 Málaga, Spain*

Available online 24 January 2006

Abstract

Catalysts based on cobalt–iridium supported on zirconium-doped mesoporous silica, with a Si/Zr molar ratio of 5, a cobalt loading of 16 wt.% and Co/Ir molar ratios of 10, 20, 30 and 60 were prepared by impregnation, characterised and then tested in the selective catalytic reduction of NO with ammonia in an excess of oxygen. These catalysts are active in the targeted catalytic reaction showing high conversions of NO at low reaction temperatures with a low yield of N₂O. The incorporation of iridium increases the dispersion of cobalt, thus improving the catalytic performance. These catalysts maintain their activities when water is added to the feed on stream, but are less active with the addition of 100 ppm of SO₂.

© 2005 Elsevier B.V. All rights reserved.

Keywords: NO; Selective catalytic reduction; Iridium; Cobalt; SO₂; XPS; NO-TPD; Mesoporous silica; Zirconium

1. Introduction

One of the main environmental problems that concerns the scientific community today is related to nitrogen oxides (NO_x) emitted into the atmosphere. NO_x is one of the most harmful pollutants involved in acid rain as well as playing a major role in the formation of tropospheric ozone with volatile organic compounds, etc. N₂O is responsible for global warming and the destruction of stratospheric ozone. Restrictive legislation has led to the control of these emissions around the world [1].

NO is produced during combustion processes by the oxidation of atmospheric nitrogen at very high temperatures. Some NO is also formed by oxidation of nitrogen compounds present in fuel [2]. Thus, NO formation may be controlled either by improving the combustion process or by reducing its concentration in the flue-gases. The latter can be achieved with catalytic technology such as the selective catalytic reduction (SCR), where a reductant such as ammonia [3,4], CO [5,6] or hydrocarbons [7,8] are necessary to convert NO into N₂. Nowadays, for stationary sources of emission, the only available method to reduce the NO concentration in waste gases on an industrial scale is the SCR of NO with ammonia. Recently, much effort has been devoted to replacing ammonia with hydrocarbons [9–11],

but an active catalyst for industrial applications has not yet been obtained. The most commonly used catalysts are based on mixed oxides: V₂O₅–WO₃–TiO₂ for the SCR of NO with ammonia. However, these catalysts suffer from some disadvantages: their activity is highest at temperatures above 250 °C, the toxicity of vanadium, etc. For these reasons, over recent decades, many research groups have been studying other systems for supports and active phases which are effective in the SCR of NO with ammonia. Research has been carried out on catalysts based on zeolites [12,13], SiO₂ [14], Al₂O₃ [15,16], etc., and on others loaded with different metals such as Fe [13,14], Cu [12,17], Cr [18,19] or Mn [15,20].

Since Li and Armor [21] reported that Co-catalysts could reduce the NO to nitrogen with methane in the presence of oxygen, the use of cobalt as an active phase has been limited mainly to the presence of methane as a reductant. Other catalysts are also active in the catalytic reduction of NO with methane such as Ga [22], Ir [23] or Pd [24]. However, the Co-catalysts are not stable in the presence of water vapour or SO₂ [25,26]. To overcome these undesired effects, bimetallic catalysts have been synthesised and tested in the SCR of NO with hydrocarbons. Supported bimetallic catalysts are of great interest because one metal can tune or modify the catalytic properties of another as a result of both electronic and structural influences. Normally, the second metal added to the Co-catalyst is a noble metal such as Pd [27] or Pt [28]. The presence of Pt or Pd appears to produce an increase in the amount of NO adsorbed, and may also

* Corresponding author. Tel.: +34 952 131876; fax: +34 952 137431.
E-mail address: ajimenezl@uma.es (A. Jiménez-López).

be responsible for NO oxidation to NO₂ (an important reaction intermediate for HC-SCR) and water tolerance. Nevertheless, the Co-catalysts have not been tested in depth in the SCR of NO with ammonia. There are only a few reports based on co-catalysts [29–31] giving worse results than those reported when methane is used as a reductant. Chmielarz et al. [32] found that a titania-pillared montmorillonite exchanged with cobalt achieved a NO conversion close to 100% at temperatures higher than 400 °C, whilst displaying high selectivities towards nitrogen. Co-ZSM-5 catalysts prepared with different methods have been assayed with *iso*-butane as reductant showing high yield of nitrogen at low temperature for catalysts containing Co²⁺oxo-ions or Co₃O₄ clusters [33].

Recently, catalysts based on iridium have received much more attention since they exhibit high activity in the reduction of NO in excess oxygen [34,35] with different reductant agents. Ogura et al. [36] reported that Ir-silicate exhibits high activity for the NO–CO reaction. Wang et al. [37] have reported that Ir-ZSM-5 monoliths could efficiently reduce NO with CO under lean conditions. Yoshinari et al. [38] reported that Ir–SiO₂ showed excellent activity for NO reduction with hydrogen in the presence of O₂ and SO₂. Moreover, several authors have emphasised the promotional effect of SO₂ present in the feed stream [38,39].

Our previous work related to Co-catalysts [40] used in the SCR of NO with ammonia showed that cobalt could be an excellent active phase with high activities and selectivity towards nitrogen. In order to improve its catalytic activity in the presence of water vapour and SO₂ in the feed stream, iridium has been selected as the promoter because the presence of iridium may improve the catalytic activity of the cobalt catalyst by increasing the dispersion of cobalt oxides and therefore the number of active sites. Thus, a family of Co/Ir catalysts supported on a zirconium doped-mesoporous silica with a Si/Zr molar ratio of 5 was prepared with a view to testing its catalytic activity in the SCR of NO with ammonia in the presence of water vapour and SO₂.

2. Experimental

2.1. Preparation of catalysts

A zirconium-doped mesoporous silica, with a Si/Zr molar ratio of 5, was prepared by following the method described in previous papers [41,42]. The material was calcined at 550 °C (1 °C min⁻¹ heating rate) for 6h and was denoted as SiZr5. This material was used as a support with a cobalt loading of 16 wt.% and Co/Ir atomic ratios of 10, 20, 30 and 60 which were prepared by the incipient wetness method. Both metals were added simultaneously to the support. After impregnation, the samples were calcined at 550 °C for 4h (1 °C min⁻¹ heating rate). For comparison, two monometallic catalysts with a cobalt loading of 16 wt.% and an iridium loading of 2 wt.% were prepared, following the same method. The monometallic catalysts were named as Co-16 and Ir-2 and the bimetallic catalysts as CoIr10, CoIr30, CoIr20 and CoIr60, depending on the Co/Ir atomic ratios.

2.2. Characterisation methods

Powder XRD patterns were obtained with a Siemens D500 diffractometer, equipped with a graphite monochromator and using Cu-K_α radiation. X-ray photoelectron spectra were collected using a Physical Electronics PHI 5700 spectrometer with non-monochromatic Mg K_α radiation (300 W, 15 kV, 1253.6 eV) for the analysis of the photoelectronic signals of Si 2p, Zr 3d, O 1s, Co 2p and Ir 4f, and equipped with a multi-channel detector. The Co 2p photoelectronic signal was collected by using a non-monochromatic Al K_α radiation (300 W, 15 kV, 1486.6 eV) as an excitation source to avoid the overlapping of the O KLL Auger line with the photoelectronic Co 2p signal. Spectra of powdered samples were recorded with the constant pass energy values at 29.35 eV, using a 720 μm diameter analysis area. During the data processing of the XPS spectra, binding energy values were referenced to the C 1s peak (248.8 eV) from the adventitious contamination layer. The PHI ACCESS ESCA-V6.0 F software package was used for acquisition and data analysis. A Shirley-type background was subtracted from the signals. Recorded spectra were always fitted using Gauss–Lorentz curves in order to determine the binding energy of the different element core levels more accurately. The error in BE was estimated to be ca. 0.1 eV.

Textural parameters were obtained from N₂ adsorption–desorption isotherms (BET method) as determined with a Micromeritics ASAP 2020. Temperature-programmed reduction of H₂ (H₂-TPR) was performed between room temperature and 800 °C using a flow of Ar/H₂ (40 cm³ min⁻¹, 10 vol.% of H₂) and a heating rate of 10 °C min⁻¹. Water produced in the reduction was eliminated by passing the gas flow through a cold finger (–80 °C). The consumption of H₂ was monitored by an on-line gas chromatograph (Shimadzu GC-14) provided with a TCD.

Temperature-programmed desorption of NO (NO-TPD) was performed by adsorbing NO onto the catalysts at room temperature (150 cm³ min⁻¹ flow rate and 0.05 vol.% NO balanced with He) for 1 h, and performing desorption between 40 and 550 °C, using a heating rate of 10 °C min⁻¹. Before the adsorption of NO, the catalysts were heated at 550 °C under a He flow for 1 h. During desorption, helium was flushed through and the eluted gas phase was carefully monitored and quantified using a Balzers GSB 300 02 on-line quadrupole mass spectrometer.

2.3. Catalysis

Catalysts were tested in the SCR of NO by using a Pyrex glass tube microreactor (6.85 mm o.d.) working at atmospheric pressure in a steady-state flow mode and with a catalytic charge of 150 mg of pelletised solids, sieved to 0.3–0.4 mm, in all cases without dilution. Samples were pretreated at 350 °C in situ for 2 h under a He flow (30 cm³ min⁻¹). The gas reaction mixture was composed of 1000 ppm NO, 1000 ppm NH₃ and 2.5 vol.% O₂ (balanced with helium). In some tests, 10 vol.% H₂O, passing helium through a saturator with deionized water and 100 ppm of SO₂, was added to the feed stream. The flows were independently controlled by channel mass flowmeters (Brooks) and a total flow rate of 42 cm³ min⁻¹ was used in the feed. The space

Table 1
Textural properties CoIr catalysts

Catalyst	Ir (%)	S_{BET} ($\text{m}^2 \text{g}^{-1}$)	Pore diameter ^a (Å)	Pore volume ^a ($\text{cm}^3 \text{g}^{-1}$)
SiZr5	–	632	33.4	0.605
Co-16	–	540	36.0	0.618
Ir-2	2.6	602	30.2	0.583
CoIr60	0.9	514	32.6	0.541
CoIr30	1.8	509	32.3	0.519
CoIr20	2.6	473	36.1	0.541
CoIr10	5.2	473	35.3	0.523

^a Determined by BJH method.

velocity (GHSV) was 3300 h^{-1} ; in these conditions, both external and internal diffusional limitations were absent. The reaction was studied from 100 to 500°C . The analysis of reactants and products (NO , N_2O , N_2 , NH_3 , H_2O and SO_2) was monitored by using the on-line quadrupole mass spectrometer described above. In previous experiments, variation in the amount of catalyst with a total flow rate maintaining the space velocity constant, produced no modification of conversion values. No influence of the particle diameter was found either.

3. Results and discussion

3.1. Characterisation of catalysts

A family of bimetallic catalysts were prepared with an atomic ratio Co/Ir of 10, 20, 30 and 60, but with the same cobalt loading of 16 wt.% supported on a zirconium doped mesoporous silica. Moreover, two monometallic catalysts with a cobalt loading of 16 wt.% and iridium loading of 2 wt.% were synthesised for comparison. Table 1 summarises the textural properties of the support and catalysts obtained from the adsorption–desorption isotherms of nitrogen. From the textural data, one can conclude that the cobalt loading causes a decrease in the specific surface area of the monometallic catalyst by blocking the mesopores. This is due to the formation of cobalt spinel particles resulting from calcination of the catalyst at 550°C , as shown in Fig. 1. The iridium loading does not affect the textural properties of the monometallic catalyst in spite of the XRD data showing intense diffraction peaks for IrO_2 [38,43] (Fig. 1), at 2θ angles of 28° , 34.3° , 40.1° and 53.8° corresponding to the 110, 101, 200 and 211 planes of IrO_2 . The textural properties of bimetallic catalysts show also a moderate decrease as the iridium loading is increased. However, the XRD patterns indicate that the diffraction peaks of IrO_2 are only observed for an iridium loading corresponding to a Co/Ir atomic ratio lower than 20. Furthermore, the diffraction peaks characteristic of Co_3O_4 appear, corresponding to the 220, 311 and 400 planes. The presence of iridium also provokes a slight broadening of the Co_3O_4 signals indicating a smaller size of the cobalt particles on the support for the bimetallic catalysts than those of monometallic ones.

In general TPR- H_2 of cobalt supported catalysts show that the two-step reduction of Co_3O_4 (via CoO) to cobalt metal can be seen either as a single peak or two resolved peaks in TPR stud-

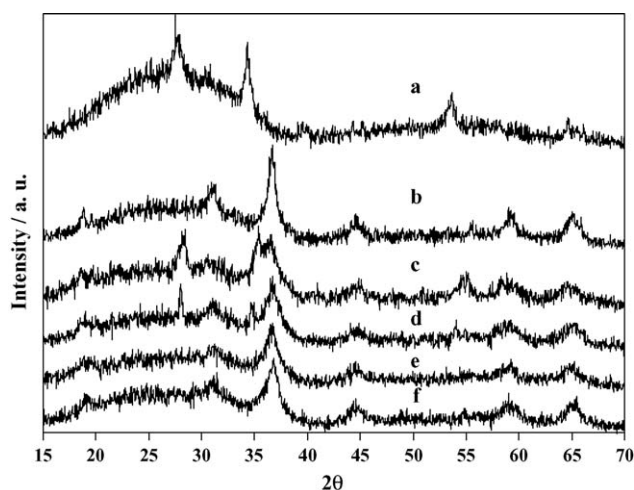


Fig. 1. Powder XRD patterns of (a) Ir-2, (b) Co-16, (c) CoIr10, (d) CoIr20, (e) CoIr30 and (f) CoIr60.

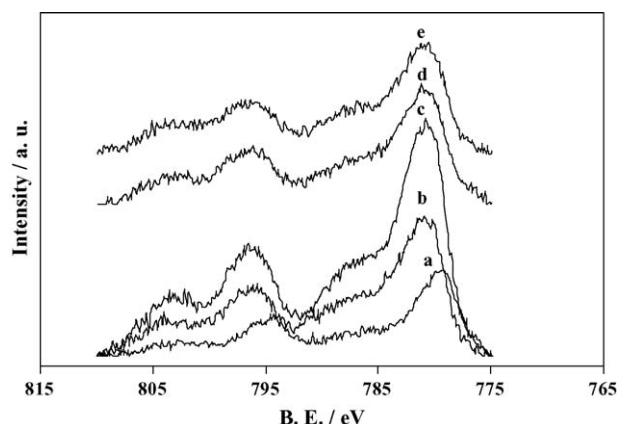


Fig. 2. Core level Co 2p XPS spectra of (a) fresh Co-16, (b) fresh CoIr60, (c) fresh CoIr30, (d) fresh CoIr20 and (e) fresh CoIr10 catalysts.

ies [44,45]. The TPR- H_2 plots of monometallic and bimetallic catalysts are shown in Fig. 2. It can be observed that the Co-16 catalyst (Fig. 2A) shows two peaks of H_2 consumption; one peak centred at 324°C with a shoulder at 294°C and a broad band from 382 to 730°C . The peak at 324°C with the shoulder at 294°C would correspond to the reduction of Co_3O_4 to metallic cobalt whereas the broad band at high temperatures might be ascribed to CoO interacting with the support with a different intensity [46] or to the presence of particles of different sizes [44]. However, the formation of cobalt silicate during calcination or the TPR test [46] by reaction of highly dispersed CoO with the silica cannot be ruled out.

The monometallic iridium catalyst shows a TPR- H_2 profile (Fig. 2B), in which the presence of a very small and negative peak at 90°C can be observed due to a small desorption of hydrogen from the metallic iridium, formed during calcination, and a broadened peak of hydrogen consumption at 220°C . There is also another small peak at 290°C . These peaks of hydrogen consumption either result from the reduction of IrO_x particles which are interacting to a different extent with the support, or IrO_x particles trapped in the pores of the support delay their reduction by

hydrogen. This point was noticed by Reyes et al. [47] together with the presence of several reduction peaks for iridium supported catalysts depending on the support used. Carnevillier et al. [48] claimed that the reduction of 0.6 wt.% Ir supported on Al_2O_3 , took place in two peaks; the reduction of large Ir particles at low temperatures, whereas the well-dispersed iridium particles were reduced at higher temperatures.

The bimetallic catalysts show quite different TPR patterns to the monometallic ones (Fig. 2C). Firstly, the small peak of IrO_2 reduction in the single iridium catalyst appears now with a very high intensity, meaning that the reduction of Ir(IV) is simultaneous to that of a fraction of cobalt. Therefore, the addition of iridium to the cobalt supported catalyst leads to the cobalt oxides undergoing reduction at lower temperatures. Thus, the reduction peak appearing at 324 °C for the Co-16 catalyst shifts towards lower temperatures (150–200 °C) in mixed oxides. Moreover, the intensity of this peak increases depending on the Co/Ir atomic ratio, suggesting that the reduction of Co_3O_4 is favoured by the presence of iridium. This means that cobalt and iridium ions are present in the vicinity and influence the reducibility of the cobalt spinel. However, the formation of lower cluster size of Co_3O_4 spinel due to the presence of iridium could also be responsible of this better reducibility of cobalt species. At the same time, the broad band at high temperatures of the Co-16 catalyst is narrowed and ranges between 200 and 450 °C. This peak is assigned to the reduction of Co^{2+} to Co^0 , indicating that the reduction of the species interacting more strongly with the support is also favoured by the presence of iridium. The promoter effect of some metals [44,49–51] on the reducibility of cobalt oxides has been reported previously by other authors. For example, Pt, Ru and Re increase the reducibility of CoO_x , although this phenomena is not accompanied by an increased dispersion of CoO_x particles.

The XPS technique is a useful tool for identifying the oxidation state of a dispersed metal oxide. XPS has been widely used to determine the presence of either Co^{2+} or Co_3O_4 over supported cobalt catalysts [46,52,53]. Owing to the small BE difference and band broadening of the Co 2p_{3/2} signal, the position of the Co 2p band alone proved unreliable for detecting the unambiguous presence of Co^{2+} or Co^{3+} . However, the Co^{2+} ion may be distinguished by the presence of a shake-up satellite and its separation from the photoelectronic band [54–56]. Moreover, the doublet separation between the 2p_{3/2} and 2p_{1/2} signals may be a parameter which could indicate the presence of Co^{2+} or Co^{3+} [54,57].

The most valuable data from the XPS spectra are shown in Table 2. The Co-16 catalyst shows a BE corresponding 2p_{3/2} of 779.5 eV as well as a low intensity shake-up satellite at 786.5 eV (Fig. 3). These features are characteristic of the presence of $\text{Co}^{2+}/\text{Co}^{3+}$ in the Co_3O_4 [46]. As the iridium is added to the Co16 catalyst, a shift is observed of the 2p_{3/2} towards a higher BE, however, this shift is unaffected by iridium loading (Fig. 3). Moreover, the intensity of the shake-up satellite is increased, reaching the highest value for the CoIr60 and CoIr30 catalysts and it then decreases for higher iridium loading. The doublet separation between the 2p_{3/2} and 2p_{1/2} is also increased with iridium loading by as much as 15.5 eV for the CoIr60 and CoIr30 cat-

alysts. This value is between 15 eV for Co_3O_4 and 15.9 eV for CoO [54,56–58]. These features seem to indicate the presence of both Co_3O_4 and Co^{2+} species dispersed over the support, the presence of Co^{2+} being higher for the CoIr60 and CoIr30 catalysts. Therefore, it would seem that the presence of iridium ions could impede the oxidation of Co^{2+} to form cobalt spinel during the calcination process. For the atomic ratios obtained by XPS (Table 2), the Co/Si ratio is increased with the iridium loading up to the CoIr30 catalyst which was also the catalyst with the highest presence of cobalt species, as observed above.

The XPS spectra in the iridium region have also been recorded. Fig. 4A corresponds to the spectrum of CoIr30, where the features of IrO_2 are observed (4f_{7/2} ca. 62.0 eV) [47,59,60] as was detected by XRD patterns, and a very low intensity doublet with a 4f_{7/2} at 61.0 assigned to Ir^0 . A Co3p photoemission also occurs in the region at 60.4 eV. The spectrum for Ir-2 catalyst shows features characteristic of Ir^0 (60.9 eV) and Ir^{4+} (61.7 eV)

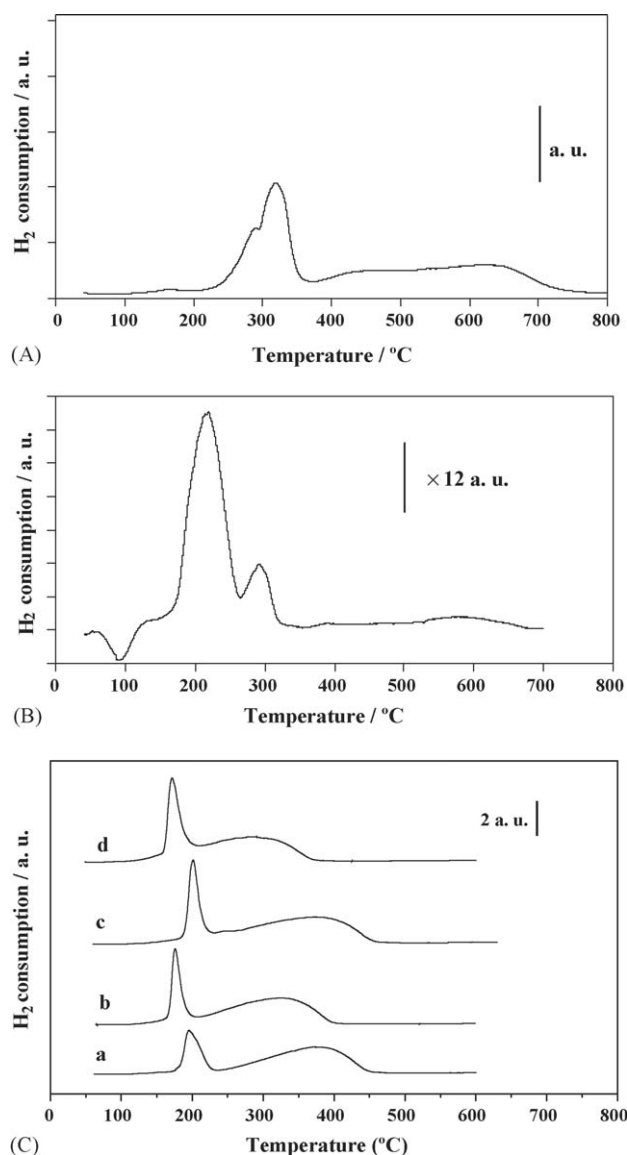


Fig. 3. (A) H₂-TPR curves of Co-16. (B) H₂-TPR curves of Ir-2. (C) H₂-TPR curves of (a) CoPt60, (b) CoIr30, (c) CoIr20 and (d) CoIr10.

Table 2
XPS data of CoIr catalysts

Catalyst	Co 2p _{3/2}	Co 2p _{1/2}	ΔE_{2p}	I_{sat} (%)	Co/Si	Ir/Co	Ir/Si	S (%)
Co-16								
Fresh	779.5	794.5	15.0	20.34	0.066	–	–	–
SO ₂	781.0	796.2	15.2	31.88	0.091	–	–	0.34
Ir-2								
Fresh	–	–	–	–	–	–	0.006	–
SO ₂	–	–	–	–	–	–	0.003	0.40
CoIr60								
Fresh	780.9	796.5	15.6	30.01	0.065	0.067	0.004	–
SO ₂	781.5	797.0	15.5	n.c.	0.075	0.010	0.005	0.48
CoIr30								
Fresh	780.7	796.2	15.5	30.45	0.086	0.106	0.007	–
SO ₂	782.1	797.5	15.4	36.06	0.070	0.104	0.005	0.57
CoIr20								
Fresh	780.9	796.0	15.1	28.78	0.047	0.087	0.006	–
SO ₂	781.4	796.6	15.2	33.54	0.077	0.135	0.007	0.45
CoIr10								
Fresh	780.9	796.1	15.2	27.79	0.051	0.157	0.007	–
SO ₂	781.4	796.9	15.5	31.99	0.086	0.223	0.015	0.49

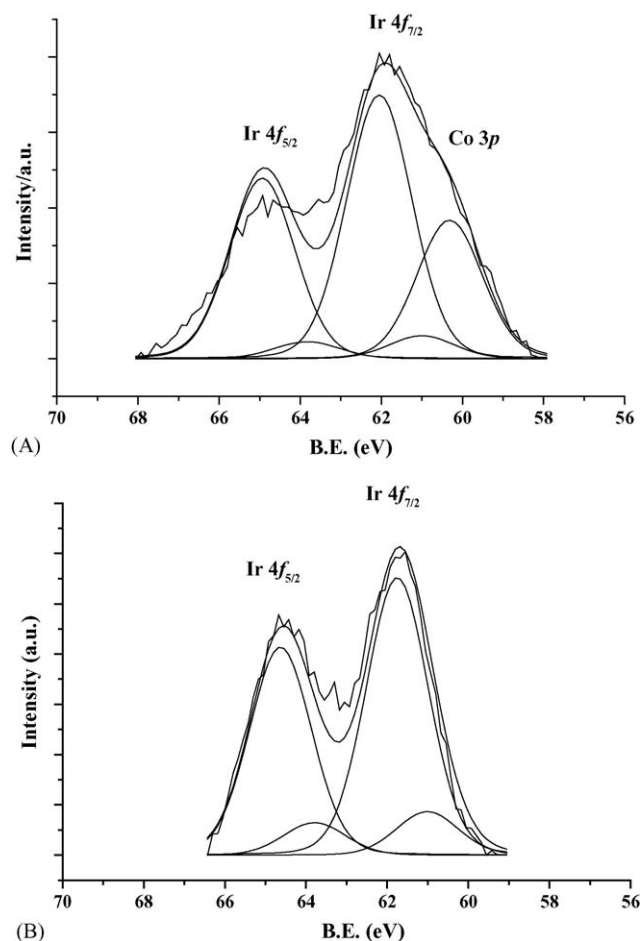


Fig. 4. Core level Ir 4f XPS spectra of (A) fresh CoIr30 and (B) fresh Ir-2.

(Fig. 4B). These results are in accordance with the XRD patterns, which only show the reflection peaks corresponding to IrO₂, and with TPR analysis, which in this case showed a negative peak ascribed to H₂ desorption from Ir⁰.

The TPD-NO profiles of the CoIr catalysts as well as of the Co-16 and Ir-2 catalysts are shown in Fig. 5. For the TPD-NO of the Co-16 catalyst (Fig. 5A), the TPD-NO plot shows three peaks at 150, 220 and 373 °C, the intensity of the 150 and 220 °C peaks being almost the same. Furthermore, the only nitrogenous species detected was NO together with a very small amount of N₂O at higher temperatures. These results are similar to those reported by Haneda et al. [62] for Co₃O₄ which showed a very broad NO desorption band from 100 to 300 °C with no desorption of N₂ or O₂, suggesting that the NO decomposition did not take place over Co₃O₄. Much research on the FTIR study of NO adsorption onto cobalt zeolites has been reported [62–67]. On the basis of these reports we may assign the two peaks at lower temperature to the desorption of NO from Co²⁺. The NO may be adsorbed as Co²⁺-NO or Co²⁺-(NO)₂. Although Lee et al. [63] claimed that the dispersed Co²⁺ ions in the ZSM-5 zeolite are responsible for NO adsorption instead of the cobalt oxide. Zhu et al. [67], studying the NO adsorption over Co-ZSM-5 with different exchanged-Co content, observed that at temperatures above 300 °C a band appeared which was assigned to the adsorption of NO onto Co₃O₄ as the zeolite was over-exchanged and cobalt oxides were present. Thus, the broad band at 373 °C may be due to the NO desorption from the Co₃O₄ particles dispersed over the support.

The TPD-NO of the Ir-2 catalyst (Fig. 5A) calcined at 550 °C shows a single broad band of NO desorption extending from 50 to 250 °C, indicating the existence of different interactions of NO molecules with the particles of IrO₂.

The amount of NO desorbed from the bimetallic catalysts (Fig. 5B) is considerably higher than from monometallic ones

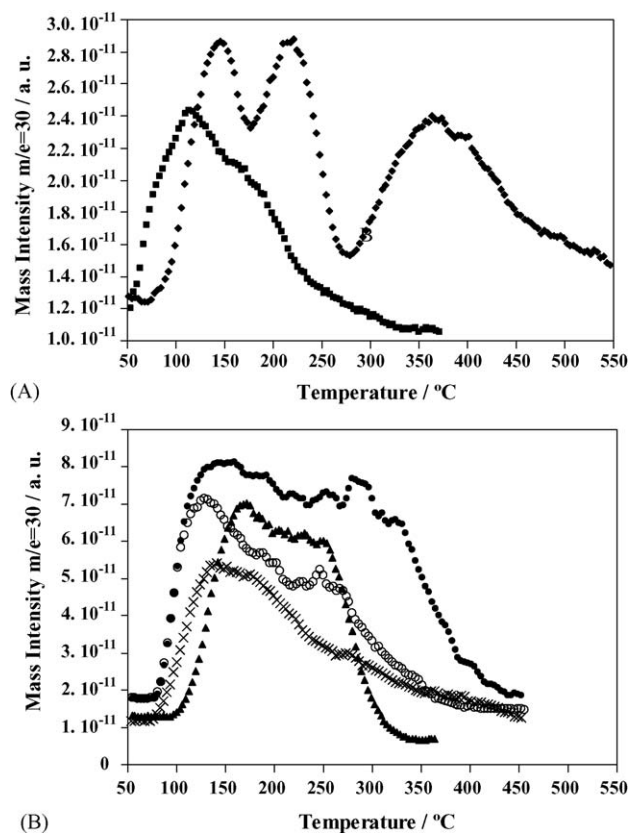
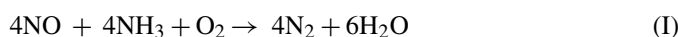


Fig. 5. (A) TPD curves of NO adsorbed on Co-16 (◆) and Ir-2 (■). (B) TPD curves of NO adsorbed on CoIr60 (▲), CoIr30 (×), CoIr20 (○) and CoIr10 (●).

in spite of all catalysts having the same cobalt loading, indicating extensive involvement of iridium on the adsorption of this molecule. Moreover, the sum of the individual amounts of desorbed NO from the monometallic catalysts does not coincide with the NO desorbed from the bimetallic catalyst and hence, there are more active sites able to adsorb NO than is the case with the monometallic catalysts, demonstrating that the presence of iridium improves the cobalt oxide dispersion over the support. This fact has been established by other authors in the case of cobalt catalysts promoted with Pd [63], alkali metals [61] or Pt [28]. CoIr60 and CoIr30, having the maximum superficial concentration of Co^{2+} ions, retain the least amount of NO, which is also desorbed at lower temperatures.

3.2. Catalytic performances

All authors currently agree that the SCR of NO with NH_3 in the presence of O_2 is based on the following reaction:



Thus, the SCR selectivity of NO with NH_3 must lead to the formation of N_2 instead of N_2O which is produced by the non-selective reaction:



Reactions (I) and (II) lead to the removal of NO, although reaction (II) must be avoided because N_2O is a harmful pollu-

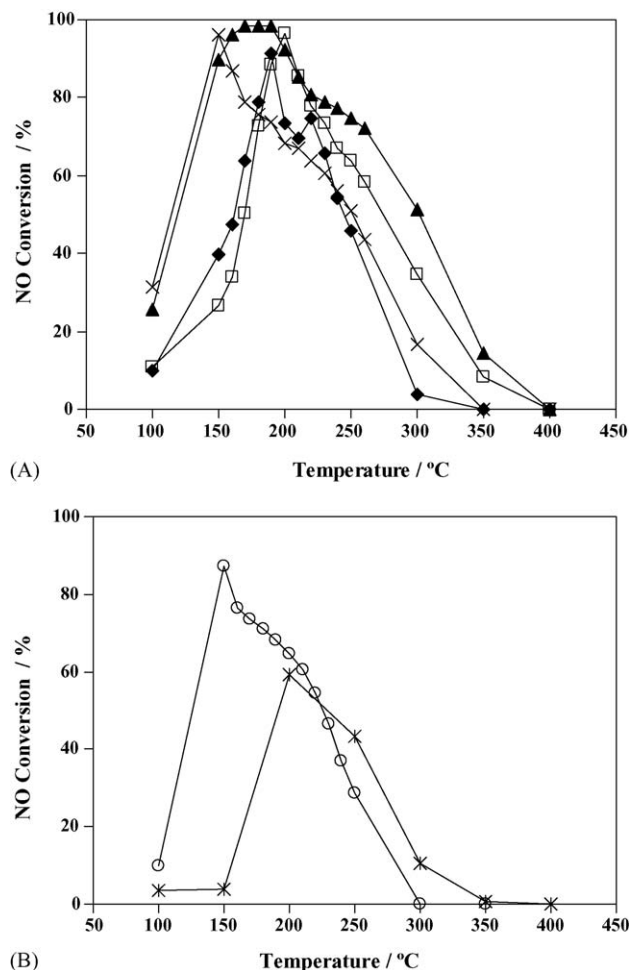


Fig. 6. (A) NO conversion as a function of reaction temperature for CoIr60 (×), CoIr30 (▲), CoIr20 (□) and CoIr10 (◆) catalysts. Experimental conditions: NO (1000 ppm), NH_3 (1000 ppm), O_2 (2.5 vol.%); total flow rate: $42 \text{ cm}^3 \text{ min}^{-1}$. (B) NO conversion as a function of reaction temperature for Co-16 (○) and Ir-2 (×) catalysts. Experimental conditions: NO (1000 ppm), NH_3 (1000 ppm), O_2 (2.5 vol.%); total flow rate: $42 \text{ cm}^3 \text{ min}^{-1}$.

tant as described above. Moreover, there are other competitive reactions in which ammonia is oxidised by the oxygen to yield N_2 , N_2O or NO.

These reactions are:



These reactions lead to ammonia consumption and therefore they are undesirable since the reductant is consumed by oxygen instead of NO.

The synthesised catalysts have been tested in the SCR of NO with ammonia in the presence of excess oxygen. Fig. 6A and B show the NO conversion of both bimetallic and monometallic catalysts in the absence of water and SO_2 in the feed. All the bimetallic catalysts (Fig. 6A) show a very similar catalytic behaviour with high activity at low temperature, with the CoIr30 catalyst reaching the highest NO conversion (98%) between 170

and 190 °C. Furthermore, for the rest of the bimetallic catalysts, the NO conversion is higher than 90%, even at 150 °C for the CoIr60 catalyst. The monometallic catalysts (Fig. 6B) show a lower NO conversion than the bimetallic ones, thus the Co-16 catalyst shows a high NO conversion at 150 °C (87%), whereas the Ir-2 catalyst only shows a 59.2% of NO conversion at 200 °C. Therefore, the addition of iridium to the Co-16 catalyst seems to be beneficial for the NO conversion with ammonia. This fact may be related to the better dispersion of the cobalt over the support as the characterisation results have shown previously. Thus, H₂-TPR revealed an easy reducibility of Co₃O₄ species due to their higher dispersion in the presence of iridium, as confirmed by XRD data. On the other hand, the catalytic performance of supported iridium catalysts is quite different when CO or hydrocarbons are used as reductant agents. Thus, Nakatsuji [68] reported NO conversions as high as 90% using propene as a reductant for 2 wt.% Ir supported on titania.

The NO conversion for each catalyst as a function of the reaction temperature show a volcano curve plot. It can be observed that the shape of the curve of the catalyst with the lowest iridium loading (the CoIr60 catalyst) is quite similar to the monometallic Co-16 catalyst although with better NO conversion, whereas the catalysts with the highest iridium loadings, the CoIr20 and CoIr10 catalysts, display curves with a shape like Ir-2, but always with a better conversion of NO. Finally, the catalyst with an intermediate iridium loading, the CoIr30 catalysts, give a different curve with a very wide temperature window of operation (120–320 °C).

The catalytic performances of this set of mixed catalysts might be related to the Co/Si atomic ratio values obtained by XPS studies. Table 2 shows the Co/Si atomic ratio for the both monometallic and bimetallic catalysts. From these data it is possible to consider Co-16 and CoIr60 as one group of catalysts and CoIr20 and CoIr10 as another, having the same Co/Si atomic

ratio, i.e. with similar cobalt dispersion over the support and hence a predictably similar catalytic performance. On the basis of the cobalt dispersion, the CoIr30 catalyst with the highest Co/Si atomic ratio value exhibits the greatest NO conversion. As regards the concentration of active centres involved in this reaction, it is again the CoIr30 which has the maximum amount of Co²⁺ ions as was shown from XPS analysis. In a previous study [40], we established that the formation of a more crystalline Co₃O₄ spinel phase on the catalysts leads to a decrease in the NO conversion. As a consequence, the presence of well dispersed Co²⁺ ions leads to the transference of oxygen from the gas phase to the catalyst and oxidation of Co²⁺ to Co³⁺, where NO is adsorbed and oxidised to NO₂. The NO₂ formed is then reduced to N₂ by ammonia. This result is in agreement with the mechanism proposed by other authors on the SCR of NO over cobalt catalysts, where the presence of CoO is necessary to catalyse the oxidation of NO to NO₂, considered as the crucial step in the performance at low temperatures [69].

Table 3 shows the catalytic data for each of the catalysts tested. There are some notable features in these results. Firstly, the ammonia is entirely consumed; this observation is notable since if the NO conversion is not 100%, then some ammonia is consumed in the non-selective reactions (reactions (III) and (IV)). This point is very important because no ammonia escapes to the atmosphere and so is not emitted as a pollutant to the environment. Secondly, the selectivity to nitrogen is higher than 92% demonstrating that reaction (I) is predominant. The exception is the Ir-2 catalyst which produces a considerable amount of N₂O and a very low selectivity to N₂, therefore making the catalyst unsuitable for the SCR of NO with ammonia. Thus, according to the catalytic data found so far, these catalysts could be candidates for the SCR of NO with ammonia and of these, CoIr30 would be the best. These results are promising because

Table 3
Catalytic data

	Catalyst	Temperature ^a (°C)	NO conversion (%)	NH ₃ conversion (%)	N ₂ O formation (ppm)	N ₂ selectivity (%)
Dry conditions	Co-16	150	87.4	100	69.0	92.4
	Ir-2	200	59.2	93.5	530.4	2.9
	CoIr60	150	96.2	99.6	55.6	94.5
	CoIr30	180	98.5	100.0	45.7	95.3
	CoIr20	200	96.5	100.0	35.5	96.3
	CoIr10	190	91.4	100.0	65.0	97.7
10% (v/v) H ₂ O	Co-16	200	83.8	83.0	30.1	96.3
	Ir-2	250	51.7	49.3	370.5	31.7
	CoIr60	200	83.2	100.0	76.6	91.0
	CoIr30	190	90.3	100.0	32.2	96.3
	CoIr20	170	51.7	50.8	88.9	83.4
	CoIr10	170	81.6	77.8	104.9	86.2
100 ppm SO ₂	Co-16	220	31.2	32.3	10.3	96.8
	Ir-2	220	8.2	12.8	105.0	0.0
	CoIr60	210	29.4	30.9	30.2	89.6
	CoIr30	200	27.3	28.2	7.9	97.1
	CoIr20	190	40.5	39.3	173.4	55.8
	CoIr10	210	49.4	55.5	186.2	62.1

^a Temperature at which the catalysts reach their highest conversion.

they are better than those reported by Lee et al. [63] for a FER exchanged with cobalt (1.47 wt.%) and iridium (0.51 wt.%) and tested in the SCR of NO with methane at a GHSV of $14,000 \text{ h}^{-1}$. These results are also an improvement on those reported previously for cobalt and platinum supported on a zirconium doped mesoporous silica [40].

When 10% (v/v) of water is added to the feed, surprisingly, the catalytic performances do not undergo substantial changes. In fact, the Co-16 catalyst exhibits only a small decrease in the NO conversion of close to 3% and even improves the selectivity to N_2 (Table 3). Only the temperature of maximum conversion is shifted to 200°C . The Ir-2 catalyst also maintains most of its catalytic activity, decreasing by only 7%, but improving the selectivity to N_2 (from 3 to 32%), although this catalyst still shows a high level of N_2O production.

In the presence of water, the bimetallic catalysts also suffer a decrease in their NO conversions, especially the CoIr20 catalyst. Among the bimetallic catalysts, the CoIr30 catalyst gives the best performance, maintaining its NO conversion at about 90% with a selectivity to N_2 close to 100% and with an ammonia conversion of 100%. It is known that water competes with NO and NH_3 for the active sites [25] on the catalyst and this is the main reason for the loss of catalytic activity. So the CoIr30 catalyst with the best dispersion is again seen to achieve the best performance.

The effect of SO_2 in the feed has also been studied. If the SO_2 concentration in the feed is 20 ppm, the CoIr10 catalyst gives a NO conversion of 72% at 220°C . The concentration of 20 ppm of SO_2 in the feed has been used by many authors to study the influence of this molecule in the catalytic activity of iridium catalysts and a promotional effect has been reported in the SCR of NO with H_2 or CO as reductant. However, when 100 ppm of SO_2 were fed to this set of catalysts, Fig. 7A and B, the activity of the catalysts is reduced, the CoIr10 catalyst giving the highest NO conversion of 49% at 210°C (Table 3). In contrast to the Ir-2 sample, which exhibits the lowest values of conversion, the catalysts with the higher cobalt loading are now the most active. This means that IrO_2 alone is not active under these experimental conditions, and there is possibly a synergic effect between Co/Ir leading to higher conversions for the CoIr10 and CoIr20 catalysts, but in both cases the N_2O formation becomes quite significant. For an insight into the influence of SO_2 in the modification of the catalytic behaviour, the spent catalysts were analysed by XPS in the Co 2p region. This peak shifted to higher B.E. values and the intensity of the shake-up satellite was increased, revealing a substantial increment in the superficial concentration of Co^{2+} ions originating from the reductant properties of SO_2 , in spite of the reaction being run in excess oxygen. On the other hand, the CoIr20 catalyst exhibits a new peak in the Ir region corresponding to Ir^0 . Thus, the presence of SO_2 increases the superficial concentration of Co^{2+} ions and impedes the formation of the $\text{Co}^{2+}/\text{Co}^{3+}$ pairs to such an extent that there is a lower NO conversion. On the other hand, by XPS is detected the presence of sulphur as SO_4^{2-} in the spent catalyst (Table 2), so the incorporation of SO_2 to the feed leads to sulfidation of the transition metal cation and hence it inhibits both NO and NH_3 adsorption as a previous step to catalysts reaction.

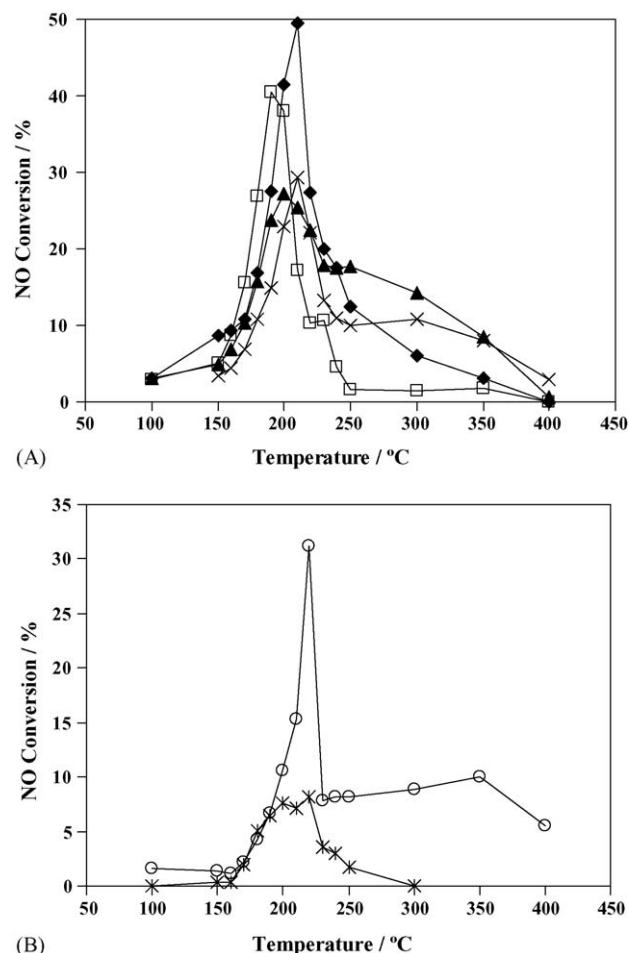


Fig. 7. (A) NO conversion as a function of temperature for CoIr60 (×), CoIr30 (▲), CoIr20 (□) and CoIr10 (◆) catalysts in the presence of 100 ppm SO_2 . Experimental conditions as mentioned in Fig. 6. (B) NO conversion as a function of temperature for Co-16 (○) and Ir-2 (×) catalysts in the presence of 100 ppm SO_2 . Experimental conditions as mentioned in Fig. 6.

4. Conclusions

Bimetallic Co–Ir catalysts supported on zirconium mesoporous silica are good catalysts for the SCR of NO by ammonia in excess oxygen at low reaction temperatures, with a high selectivity to N_2 and a very low selectivity to N_2O . The reductant agent, NH_3 , was totally converted. The incorporation of iridium has a beneficial effect promoting the reducibility and the dispersion of cobalt oxides and reducing the formation of the cobalt spinel during the calcination process. The addition of water to the feed does not produce significant changes in the catalytic performance. However, the presence of 100 ppm pf SO_2 in the feed produces a dramatic decrease of the catalytic activity probably due to an increase of the superficial Co^{2+} concentration originating from the reducing properties of SO_2 .

Acknowledgement

Financial support from the European Brite/EuRam Contract BRPR-CT97-0545 is acknowledged with thanks.

References

- [1] R.V. Pouyat, M.A. McGlinch, *Environ. Sci. Policy* 1 (1998) 249.
- [2] G. Busca, L. Lietti, G. Rams, F. Berti, *Appl. Catal. B* 18 (1998) 1.
- [3] I.E. Wachs, G. Deo, B.M. Weckhuysen, A. Andreini, M.A. Vuurman, M. De Boer, M.D. Amiridis, *J. Catal.* 161 (1996) 211.
- [4] L. Lietti, *Appl. Catal. B* 10 (1996) 281.
- [5] M. Meng, P.-Y. Lin, Y.-L. Fu, *Catal. Lett.* 48 (1997) 213.
- [6] M. Antunes Pereira da Silva, M. Schmal, *Catal. Today* 85 (2003) 31.
- [7] Z. Chajar, V. Le Chanu, M. Primet, H. Praliaud, *Catal. Lett.* 52 (1998) 97.
- [8] H.K. Shin, H. Hirabayashi, H. Yahiro, M. Watanabe, M. Iwamoto, *Catal. Today* 26 (1995) 13.
- [9] A.D. Cowan, R. Dümpelmann, N.W. Cant, *J. Catal.* 151 (1995) 356.
- [10] H.Y. Chen, T. Voskoboinikov, W.M.H. Sachtler, *Catal. Today* 54 (1999) 483.
- [11] B.K. Cho, J.E. Yie, *Appl. Catal. B* 10 (1996) 263.
- [12] W. Wang, S.J. Hwang, *Appl. Catal. B* 5 (1995) 187.
- [13] R.Q. Long, R.T. Yang, *Catal. Lett.* 74 (2001) 201.
- [14] P. Fabrizioli, T. Bürgi, A. Baiker, *J. Catal.* 206 (2002) 143.
- [15] W.S. Kijlstra, D.S. Brands, E.K. Poels, A. Blik, *Catal. Today* 50 (1999) 133.
- [16] G. Centi, S. Perathoner, D. Biglino, E. Giamello, *J. Catal.* 151 (1995) 75.
- [17] G. Delahay, B. Coq, S. Kieger, B. Neveu, *Catal. Today* 54 (1999) 431.
- [18] B.L. Duffy, H.E. Curry-Hyde, N.W. Cant, P.F. Nelson, *J. Catal.* 154 (1995) 107.
- [19] H. Schneider, M. Maciejewski, K. Köhler, A. Wokaun, A. Baiker, *J. Catal.* 157 (1995) 312.
- [20] L. Chmielarz, R. Dziembaj, T. Grybek, J. Klinik, T. Lojewski, D. Olszewska, H. Papp, *Appl. Catal. Lett.* 68 (2000) 95.
- [21] Y. Li, J.N. Armor, *Appl. Catal. B* 13 (1992) L31.
- [22] Y. Li, J.N. Armor, *J. Catal.* 145 (1994) 1.
- [23] H. Ohtsuka, *Appl. Catal. B* 33 (2001) 325.
- [24] Y.K. Park, J.W. Lee, C.W. Lee, S.E. Park, *J. Mol. Catal. A* 158 (2000) 173.
- [25] Y. Li, P.J. Battavio, J.N. Armor, *J. Catal.* 142 (1993) 561.
- [26] P. Budi, R.F. Howe, *Catal. Today* 38 (1997) 175.
- [27] B. Wen, J. Jia, S. Li, T. Liu, L.X. Chen, W.M.H. Sachtler, *Phys. Chem. Chem. Phys.* 4 (2002) 1983.
- [28] L. Gutierrez, A. Boix, J.O. Petunchi, *J. Catal.* 179 (1998) 179.
- [29] D.A. Peña, B.S. Uphade, P.G. Smirniotis, *J. Catal.* 221 (2004) 421.
- [30] M. Brandhorst, J. Zajac, D.J. Jones, J. Rozière, M. Womes, A. Jiménez-López, E. Rodríguez Castellón, *Appl. Catal. B* 55 (2005) 267.
- [31] L. Chmielarz, P. Kustrowski, A.R. Lasocha, D. Majda, R. Dziembaj, *Appl. Catal. B* 35 (2002) 195.
- [32] L. Chmielarz, P. Kustrowski, M. Zbroja, B. Gil-Kanp, J. Datka, R. Dziembaj, *Appl. Catal. B* 45 (2003) 103.
- [33] X. Wang, H.-Y. Chen, W.M.H. Sachtler, *Appl. Catal. B* 26 (2000) L227.
- [34] C. Wögerbauer, M. Maciejewski, A. Baiker, *Appl. Catal. B* 34 (2001) 11.
- [35] C. Wögerbauer, M. Maciejewski, A. Baiker, U. Göbel, *Topics Catal.* 16–17 (2001) 181.
- [36] M. Ogura, A. Kawamura, M. Matsukata, E. Kikuchi, *Chem. Lett.* (2000) 146.
- [37] A. Wang, D. Liang, C. Xu, X. Sun, T. Zhang, *Appl. Catal. B* 32 (2001) 205.
- [38] T. Yoshinari, K. Sato, M. Haneda, Y. Kintaichi, H. Hamada, *Appl. Catal. B* 41 (2003) 157.
- [39] T. Yoshinari, K. Sato, M. Haneda, Y. Kintaichi, H. Hamada, *Catal. Commun.* 2 (2001) 155.
- [40] R. Moreno-Tost, J. Santamaría-González, P. Maireles-Torres, E. Rodríguez-Castellón, A. Jiménez-López, *Appl. Catal. B* 38 (2002) 51.
- [41] D.J. Jones, J. Jiménez-Jiménez, A. Jiménez-López, P. Maireles-Torres, P. Olivera-Pastor, E. Rodríguez-Castellón, J. Rozière, *Chem. Commun.* (1997) 431.
- [42] E. Rodríguez-Castellón, A. Jiménez-López, P. Maireles-Torres, D.J. Jones, J. Rozière, M. Trombetta, G. Busca, M. Lenarda, L. Storaro, *J. Solid State Chem.* 175 (2003) 159.
- [43] M. Haneda, Y. Pusparatu, I. Kintaichi, M. Nakamura, T. Sasaki, H. Fujitani, Hamada, *J. Catal.* 229 (2005) 197.
- [44] D. Schanke, S. Vada, E.A. Blekkan, A.M. Hilmen, A. Hoff, A. Holmen, *J. Catal.* 156 (1995) 85.
- [45] S. Sun, N. Tsubaki, K. Fujimoto, *Appl. Catal. A* 202 (2000) 121.
- [46] A. Martínez, C. López, F. Márquez, I. Díaz, *J. Catal.* 220 (2003) 486.
- [47] P. Reyes, M.C. Aguirre, G. Pecchi, J.L.G. Fierro, *J. Mol. Catal. A* 164 (2000) 245.
- [48] C. Carnevillier, F. Epron, P. Marecot, *Appl. Catal. A* 275 (2004) 25.
- [49] S.A. Hosseini, A. taeb, F. Feyzi, F. Yaripour, *Catal. Commun.* 5 (2004) 137.
- [50] W.S. Epling, P.K. Cheekatamarla, A.M. Lane, *Chem. Eng. J.* 93 (2003) 61.
- [51] G. Jacobs, T.K. Das, Y. Zhang, J. Li, G. Racoillet, B.H. Davis, *Appl. Catal. A* 233 (2002) 263.
- [52] Y. Okamoto, K. Nagata, T. Adachi, T. Imanaka, K. Inamura, T. Tayku, *J. Phys. Chem.* 95 (1991) 310.
- [53] A.Y. Khodakov, A. Griboval-Constant, R. Bechara, V.L. Zholobenko, *J. Catal.* 206 (2002) 230.
- [54] D. Pietrogiamici, S. Tuti, M.C. Campa, V. Indovina, *Appl. Catal. B* 28 (2000) 43.
- [55] G. Fierro, M.A. Eberhardt, M. Houalla, D.M. Hercules, W.K. Hall, *J. Phys. Chem.* 100 (1996) 8468.
- [56] A. Frydman, D.G. Castner, M. Schmal, C.T. Campbell, *J. Catal.* 152 (1995) 164.
- [57] N. Li, A. Wang, M. Zheng, X. Wang, R. Cheng, T. Zhang, *J. Catal.* 225 (2004) 307.
- [58] Y. Brik, M. Kacimi, M. Ziyad, F. Bozon-Verduraz, *J. Catal.* 202 (2001) 118.
- [59] H. Tian, T. Zhang, X. Sun, D. Liang, L. Li, *Appl. Catal. A* 210 (2001) 55.
- [60] K. Nakagawa, N. Ikenaga, T. Suzuki, T. Kobayashi, M. Haruta, *Appl. Catal. A* 169 (1998) 281.
- [61] L.A. Silva, V.A. Alves, S.C. de Castro, J.F.C. Boodts, *Colloids Surf. A: Physicochem. Eng. Aspects* 170 (2000) 119.
- [62] M. Haneda, Y. Kintaichi, N. Bion, H. Hamada, *Appl. Catal. B* 46 (2003) 473.
- [63] C.W. Lee, P.J. Chong, Y.C. Lee, C.S. Chin, L. Kewan, *Micropor. Mater.* 12 (1997) 21.
- [64] T.J. Lee, I.-S. Nam, S.-W. Ham, Y.-S. Baek, K.-H. Shin, *Appl. Catal. B* 41 (2003) 115.
- [65] K. Hadjiivanov, B. Tsyntsarski, T. Nikolova, *Phys. Chem. Chem. Phys.* 1 (1999) 4521.
- [66] F. Geobaldo, B. Onida, P. Rivolo, F. Di Renzo, F. Fajula, E. Garrone, *Catal. Today* 70 (2001) 107.
- [67] C.Y. Zhu, C.W. Lee, P.J. Chong, *Zeolites* 17 (1996) 483.
- [68] T. Nakatsuji, *Appl. Catal. B* 25 (2000) 163.
- [69] A.Y. Stakheev, C.W. Lee, S.J. Park, P.J. Chong, *Catal. Lett.* 38 (1996) 327.